

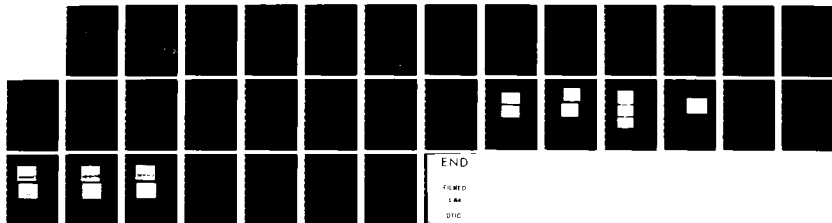
AD-A135 589

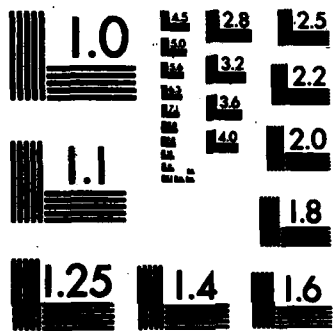
EXPERIMENTS WITH ACTIVE PHASE MATCHING OF  
PARALLEL-AMPLIFIED MULTILINE HF. (U) AEROSPACE CORP EL  
SEGUNDO CA AEROPHYSICS LAB J G COFFER ET AL. 31 DEC 82  
TR-0083(3764)-1 SD-TR-82-87 F/G 20/6

1/1

UNCLASSIFIED

NL





MICROCOPY RESOLUTION TEST CHART  
NATIONAL BUREAU OF STANDARDS-1963-A

12

AD-A135 589

# Experiments with Active Phase Matching of Parallel-Amplified, Multiline HF Laser Beams by a Phase-Locked Mach-Zehnder Interferometer

J. G. COFFER, J. M. BERNARD, R. A. CHODZKO,  
E. B. TURNER, R. W. F. GROSS, and W. R. WARREN  
Aerophysics Laboratory  
Laboratory Operations  
The Aerospace Corporation  
El Segundo, Calif. 90245

31 December 1982

DTIC  
ELECTE  
DEC 8 1983  
S B

APPROVED FOR PUBLIC RELEASE;  
DISTRIBUTION UNLIMITED

DTIC FILE COPY

Prepared for  
SPACE DIVISION  
AIR FORCE SYSTEMS COMMAND  
Los Angeles Air Force Station  
P.O. Box 92960, Worldway Postal Center  
Los Angeles, Calif. 90009

This report was submitted by The Aerospace Corporation, El Segundo, CA 90245, under Contract No. F04701-82-C-0083 with the Space Division, P.O. Box 92960, Worldway Postal Center, Los Angeles, CA 90009. It was reviewed and approved for The Aerospace Corporation by W. P. Thompson, Jr., Director, Aerophysics Laboratory. Lt Steven G. Webb, SD/AFSTC (Det. 1), was the Air Force project officer.

This report has been reviewed by the Public Affairs Office (PAS) and is releasable to the National Technical Information Service (NTIS). At NTIS, it will be available to the general public, including foreign nationals.

This technical report has been reviewed and is approved for publication. Publication of this report does not constitute Air Force approval of the report's findings or conclusions. It is published only for the exchange and stimulation of ideas.

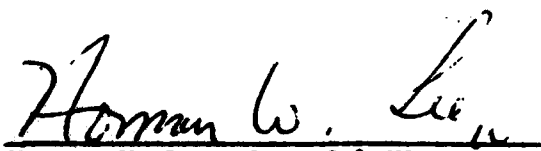


Steven G. Webb, 1st Lt, USAF  
Project Officer



David T. Newell, Lt Colonel, USAF  
Acting Director, Space Systems  
Technology

FOR THE COMMANDER



Norman W. Lee, Jr., Col USAF  
Commander, Det 1, AFSTC

UNCLASSIFIED

SECURITY CLASSIFICATION OF THIS PAGE (When Data Entered)

REPORT DOCUMENTATION PAGE		READ INSTRUCTIONS BEFORE COMPLETING FORM
1. REPORT NUMBER SD-TR-82-87	2. GOVT ACCESSION NO. AD-A135587	3. RECIPIENT'S CATALOG NUMBER
4. TITLE (and Subtitle) EXPERIMENTS WITH ACTIVE PHASE MATCHING OF PARALLEL-AMPLIFIED, MULTILINE HF LASER BEAMS BY A PHASE-LOCKED MACH-ZEHNDER INTERFEROMETER		5. TYPE OF REPORT & PERIOD COVERED
7. AUTHOR(s) John G. Coffey, Jay M. Bernard, Richard A. Chodzko, Eugene B. Turner, Rolf W. F. Gross, and Walter R. Warren		6. PERFORMING ORG. REPORT NUMBER TR-0083(3764)-1
9. PERFORMING ORGANIZATION NAME AND ADDRESS The Aerospace Corporation El Segundo, Calif. 90245		8. CONTRACT OR GRANT NUMBER(s) F04701-82-C-0083
11. CONTROLLING OFFICE NAME AND ADDRESS Space Division Air Force Systems Command Los Angeles, Calif. 90009		10. PROGRAM ELEMENT, PROJECT, TASK AREA & WORK UNIT NUMBERS
14. MONITORING AGENCY NAME & ADDRESS (if different from Controlling Office)		12. REPORT DATE 31 December 1982
		13. NUMBER OF PAGES 35
		15. SECURITY CLASS. (of this report) UNCLASSIFIED
		15a. DECLASSIFICATION/DOWNGRADING SCHEDULE
16. DISTRIBUTION STATEMENT (of this Report) Approved for public release; distribution unlimited		
17. DISTRIBUTION STATEMENT (of the abstract entered in Block 20, if different from Report)		
18. SUPPLEMENTARY NOTES		
19. KEY WORDS (Continue on reverse side if necessary and identify by block number)		
CW laser	Laser amplifier	Phased array
Dispersive phase mismatch	Multiline laser	Resonant dispersion
Dither COAT	Parallel MOPA	
HF chemical laser	Phase locking	
Interferometry	Phase matching	
20. ABSTRACT (Continue on reverse side if necessary and identify by block number)		
<p>Active phase matching of multiline HF laser beams by means of a phase-locked Mach-Zehnder interferometer was demonstrated by locking the interferometer to the central interference fringe at zero optical pathlength difference. The central fringe could be found by varying the spectral content of the input beam. Laser amplification in one leg of the interferometer decreased fringe visibility without adversely affecting locking. Single-line fringe patterns produced by an array spectrometer (while the interferometer was operated in</p>		

DD FORM 1473 (FACSIMILE)

UNCLASSIFIED

SECURITY CLASSIFICATION OF THIS PAGE (When Data Entered)

UNCLASSIFIED

SECURITY CLASSIFICATION OF THIS PAGE(When Data Entered)

18. KEY WORDS (Continued)

19. ABSTRACT (Continued)

its scanning mode) were analyzed to show that no significant resonant dispersion occurred in the amplifier. The techniques developed have potential for measuring dispersion mismatch between larger parallel amplifiers. These experiments demonstrated in principle that a number of multiline HF amplified beams can be recombined and phase-matched to produce a high beam-quality output beam.

UNCLASSIFIED

SECURITY CLASSIFICATION OF THIS PAGE(When Data Entered)

PREFACE

The authors wish to thank Chris Quinn for her computer programming support, Gary Segal and Gary Wiemokly for their computer assistance, Charles Wang and Robert Varwig for their invaluable technical advice, Harold Mirels for his direction, Paul Thompson for his encouragement, and Michael Meyer for his editorial guidance.

Accession For	
NTIS GRA&I	<input checked="" type="checkbox"/>
DTIC TAB	<input type="checkbox"/>
Unannounced	<input type="checkbox"/>
Justification	
By	
Distribution/	
Availability Codes	
Dist	Avail and/or Special
AI	



## CONTENTS

PREFACE.....	1
I. INTRODUCTION.....	5
II. THEORY.....	7
III. EXPERIMENTAL.....	13
IV. RESULTS.....	17
V. CONCLUSIONS.....	27
REFERENCES.....	29



## FIGURES

1.	Experimental Equipment.....	8
2.	(a) Multiline Fringe Intensities $I^+$ ( $g = 0$ ) and $I^-$ ( $g = 0$ ) Locking without Gain; (b) Multiline Fringe Intensities $I^+$ ( $g$ ) and $I^-$ ( $g$ ) Locking with Gain (amplifier on).....	18
3.	(a) Chopping of Control Loop and Attainment of Locking; (b) Locking on Two Different Fringes.....	19
4.	(a) Induced Line Switching (ILS) Analyzed; (b) Effect of ILS at Zero OPD; (c) Effect of ILS off Zero OPD.....	20
5.	Comparison of Rotating Grating with Array Spectrometer.....	21
6.	Scan of Multiline Interference Fringes through Zero OPD, Laser Amplifier Power Off.....	23
7.	Scan of Multiline Interference Fringes through Zero OPD, Laser Amplifier Power On.....	24
8.	Scan of Multiline Interference Fringes through Zero OPD, Laser Amplifier Power On.....	25

## TABLE

1.	Calibration Coefficients $C_1$ .....	22
----	--------------------------------------	----

## I. INTRODUCTION

Earlier work<sup>1</sup> showed that a clear, high-visibility, central fringe was observable in interference patterns of multiline HF laser radiation when these patterns were produced by a scanning Mach-Zehnder interferometer (MZ). The purpose of the work was to explore questions raised in a parallel multiline laser-amplifier phase-matching proposal.<sup>2</sup> A demonstration of active, temporal phase matching of two amplified, multiline HF laser beams was desired. This meant locking the interferometer to the central fringe.

In the present work two superposed multiline HF laser beams in the direct exit of a phase-locked MZ interferometer were actively phase-matched at zero optical path difference (OPD). The interferometer acted as the producer, phase controller, and phase analyzer of the two beams. The phase-lock system was a mirror-dither hill-climbing servo.

Phase matching of the beams in the direct exit of the MZ is a necessary condition for the MZ to produce a zero-intensity infinite fringe in its indirect exit. This indirect-exit intensity was monitored to control the servo system and evaluate the system's performance. The servo system operated electro-optically to minimize this intensity. It employed a small-amplitude oscillation, or dither, of one of the MZ mirrors and a control feedback loop to lock the MZ to an interference fringe. The response of the system was tested. A method was found to check alignment of the MZ to the central fringe while the MZ was locked.

Amplification was to be provided for only one beam, the other being considered to have zero gain. Laser amplification in one leg of the interferometer provided gain of 12% per cm (gain length  $L = 17$  cm) on some lines of the multiline beam. This did not prevent phase-locking of the interferometer. It did affect the visibility of the interference fringes in the interferometer exits so that phase-matching was no longer easily identified by a zero of intensity in the indirect exit.

Patterns of fringe intensity as a function of OPD were recorded by an array spectrometer. From the reduced visibility of these single-line patterns, gain on each line could be measured at 3-ms intervals from each fringe of a 500-ms scan. Theoretically, visibility of single-line fringe patterns should not be altered by any phase shift induced by resonant refractive index in the amplifier. Visibility of the multiline central fringe, however, should be reduced by dispersion-induced phase mismatch between the various single-line fringe patterns, as well as by single-line gains. The visibility of the multiline central fringe with gain was found to be entirely attributable to the reductions in single-line visibilities that result from gain, within experimental error. This implied that the laser amplifier used did not show a significant degree of dispersion. The technique may be applicable to measuring the degree of dispersion mismatch between two larger, parallel, multiline amplifiers.

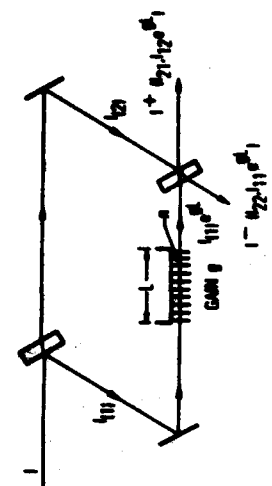
## II. THEORY

The following analysis was performed to derive expressions for intensity as a function of OPD in a MZ (Fig. 1a) when the beam splitters are 50% reflective. The intensities  $I^+$  and  $I^-$  are the interference intensities of two collinear beams in the two exits of the MZ when it is adjusted for infinite fringes (Fig. 1b). In the analysis the beam in one leg of the interferometer experiences selective amplification of some spectral lines (Fig. 1c). The direct exit is the exit whose output  $I^+$  is parallel to the input beam. The indirect exit is the exit in which one beam has suffered internal reflection as dictated by the experimental setup (Fig. 1d).

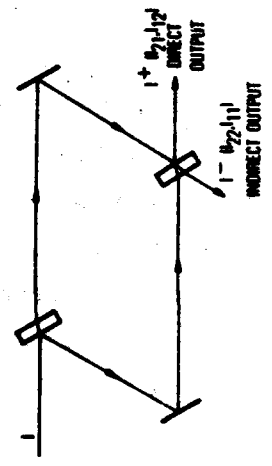
Amplification involves resonant dispersion in the amplifier medium. The analysis includes dispersion in order to describe the effect of dispersion on temporal phase matching when the parallel amplifiers used are not identical. The problem of dispersion in parallel multiline amplifiers is similar to the need for a dispersion-compensation plate in the production of white-light fringes in a Michelson interferometer.<sup>3</sup> In the parallel amplifier case, each amplifier acts as a dispersion compensator for the other. Dispersion in a laser amplifier depends on interaction of the amplifier medium with the driving oscillator beam and must be compensated by identical amplifiers driven by identical beams unless the dispersion is negligible.

Unbalanced dispersion was expected to affect phase-locking of the interferometer through its effect on central-fringe visibility. An equation is derived in the analysis to describe multiline central-fringe visibility in terms of single-line fringe intensities to compare fringe-scan data and look for evidence of dispersive phase mismatch [Eq. (17)].

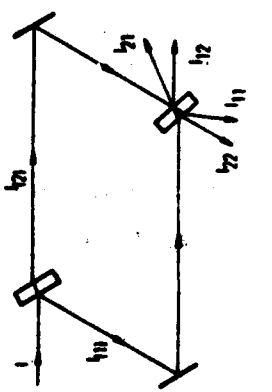
The use of collinear output beams simplified our experiments. A description of the dither system of coherent optical adaptive technique (COAT) involving spatially separated beams and their far-field spatial coherence is found in Ref. 4.



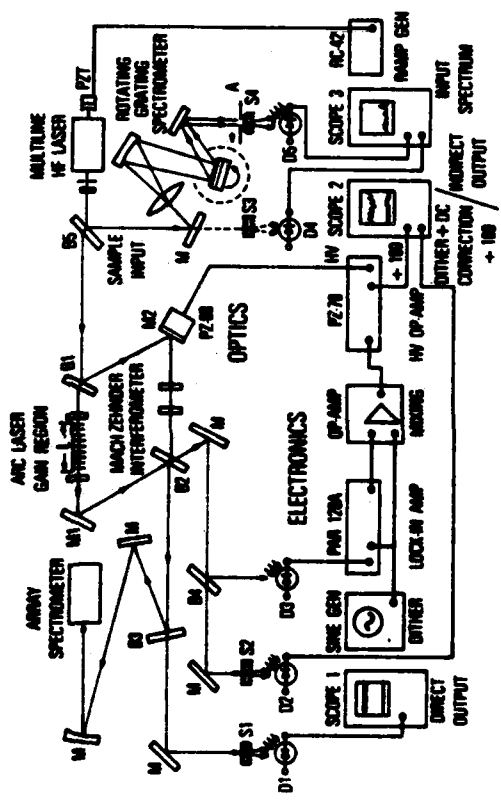
a



b



c



d

Fig. 1. Experimental Equipment

Two superposed beams of monochromatic radiation, having intensities  $I_1$  and  $I_2$  in the direct exit of the MZ, form infinite interference fringes of intensity  $I^+$ .  $I^+$  depends upon the phase difference  $\delta^+$  between the waves after they pass through the MZ.<sup>5</sup>

$$I^+ = I_1 + I_2 + 2 \sqrt{I_1 I_2} \cos \delta^+ \quad (1)$$

The phase difference  $\delta^+$  depends on the optical pathlength difference (OPD)  $X$  in the MZ. OPD becomes  $Z = X + (n - 1)L$  for a region of length  $L$  and refractive index  $n$  in one leg of the MZ if this region is not matched by a similar region in the other leg, and

$$\delta^+ = \frac{2\pi Z}{\lambda} \quad (2)$$

where  $\lambda$  is the wavelength of the radiation. Since the two beam splitters are 50% reflective,  $I_1 = I_2 = 1/4 I$ , where  $I$  is the input intensity into the MZ. Therefore,

$$I^+ = 1/2 I \left( 1 + \cos \frac{2\pi Z}{\lambda} \right) \quad (3)$$

In the indirect exit the phase of one beam is shifted by  $\pi$  rad because of internal reflection at the second beamsplitter. So

$$\delta^- = \delta^+ + \pi \quad (4)$$

Therefore, in the indirect exit

$$I^- = 1/2 I \left( 1 - \cos \frac{2\pi Z}{\lambda} \right) \quad (5)$$

Written together, Eqs. (3) and (5) are

$$I^\pm = 1/2 I \left( 1 \pm \cos \frac{2\pi Z}{\lambda} \right) \quad (6)$$

The intensity of one of the interfering beams, after experiencing gain  $g$  in the amplifier in one leg of the MZ, is

$$I_1(g) = I_1(0) e^{gL} = \frac{1}{4} I e^{gL} \quad (7)$$

Equation 6 becomes, for the case of gain in one beam,

$$I^\pm(g) = \frac{1}{4} I (1 + e^{gL} \pm 2e^{gL/2} \cos \frac{2\pi Z}{\lambda}) \quad (8)$$

Maximum intensity in either exit occurs when the cosine is ( $\pm$ ) unity:

$$I^\pm(g)_{\max} = \frac{1}{4} I (1 + e^{gL/2})^2 \quad (9)$$

Simultaneously, in the opposite exit, minimum intensity is

$$I^\mp(g)_{\min} = \frac{1}{4} I (1 - e^{gL/2})^2 \quad (10)$$

From Eqs. (9) and (10), for  $g > 0$

$$g = \frac{2}{L} \ln \frac{\sqrt{I_{\max}} + \sqrt{I_{\min}}}{\sqrt{I_{\max}} - \sqrt{I_{\min}}} \quad (11)$$

where we have dropped the  $\pm$  and ( $g$ ) notation. This permits a pointwise measurement of  $g$  from a single-line fringe-intensity scan by a calculation similar to that used for fringe visibility  $V$ , namely,

$$V = \frac{I_{\max} - I_{\min}}{I_{\max} + I_{\min}} \quad (12)$$

For multiline beams with wavelengths  $\lambda_1$ , intensities are simply additive, neglecting mode beating. Equation (6) becomes

$$I^{\pm} = \sum_i \frac{1}{2} I_i (1 \pm \cos \frac{2\pi Z_i}{\lambda_i}) \quad (13)$$

When  $\lambda_i$  experience gains  $g_i$  and refractive indices  $n_i$  in the amplifier, Eq. (8) becomes

$$I^{\pm}(g_i, n_i) = \frac{1}{4} \sum_i I_i [1 + e^{g_i L} \pm 2 e^{g_i L/2}] \cos \frac{2\pi}{\lambda_i} [X + (n_i - 1)L] \quad (14)$$

Assuming no dispersion,  $n_i = n$  for all  $i$  and

$$I^{\pm}(g_i) = \frac{1}{4} \sum_i I_i [1 + e^{g_i L} \pm 2 e^{g_i L/2}] \cos \frac{2\pi Z}{\lambda_i} \quad (15)$$

The maximum and minimum intensities occur in the direct and indirect exits, respectively, when  $Z = 0$  (zero OPD):

$$I^{\pm}(g_i)_{\substack{\text{max} \\ \text{(min)}}} = \frac{1}{4} \sum_i I_i (1 + e^{g_i L} \pm 2 e^{g_i L/2}) \quad (16)$$

Therefore the direct-output multiline maximum intensity with gain at zero OPD is still a simple sum of the single-line maximum intensities [cf Eq. (9)]. For HF lasers  $\lambda_i$  varies from  $\lambda_j$  by at most  $\frac{\lambda_j}{10}$  for all  $i, j$ . Therefore, the phase mismatch of interference patterns of  $\lambda_i$  and  $\lambda_j$  near the direct-output minimum at  $Z = \frac{\lambda}{2}$  is at most  $\frac{\pi}{10}$  rad, because of wavelength difference. This makes the direct-output multiline central-fringe minimum intensity with gain very nearly the sum of the single-line minima with gain as long as  $n_i = n$  for all  $i$ . Hence, in the absence of dispersion, the visibility  $V(Z = 0)$  of the multiline central fringe is calculable from the intensity maxima and minima of the direct-output single-line central fringes, i.e.,

$$V(Z = 0) = \frac{\sum I_{\text{max}} - \sum I_{\text{min}}}{\sum I_{\text{max}} + \sum I_{\text{min}}} \quad (17)$$

where the sums are taken over all single-line central fringes.



The above relationship does not hold true at non-zero values of OPD, simply because the various single-line patterns of fringe intensity as a function of OPD are out of phase with each other because of their unlike wavelengths. That relationship also fails to hold true for the central fringe if values of  $n_1$  are significantly unlike, but in this case the phase mismatch is caused by dispersion. A unique zero OPD does not exist simultaneously for all single-line interference patterns when some are phase-shifted relative to others. The maximum phase shift resulting from resonant dispersion in our amplifier is expected to be about  $\pm \frac{\pi}{5}$  rad, relative to the reference leg, for some lines. This means that the sine-wave interference intensity patterns of two spectral lines in the MZ could experience a phase shift of  $\frac{2\pi}{5}$  relative to one another. The addition of two such shifted patterns of equal amplitude and approximately equal wavelength would produce a decrease in their combined visibility from  $V(Z = 0) = 1.0$  to  $V = 0.81$  in the presence of dispersion. We are referring here to one amplifier with dispersion, but no gain, in one leg of the MZ [Eq. (13)]; gain would further reduce visibility [Eq. (15)].

Dispersion is always present in any optical system and we want to know its magnitude and how it affects the system. More important, for parallel amplifiers we need to know how different is the dispersion in one amplifier from that in another when both are driven by the same input function. To answer this question we constructed a system to continuously phase-match two identical beams, then successfully used that system with one beam amplified. Finally, we measured and analyzed typical single-line gains and their combined effect on multiline central-fringe visibility.

### III. EXPERIMENTAL

Figure 1d shows the complete layout of the experiments. The multiline HF probe-laser<sup>6,7</sup> was constrained to the TEM<sub>00</sub> mode by a 2-mm aperture. The laser cavity length of 50 cm permitted only one strong longitudinal mode per line. This ensured that each spectral line was essentially monochromatic. Cavity-length changes, induced by a piezoelectric transducer (PZT) driving the cavity mirror, permitted induced fluctuations in the probe-laser output-spectrum (see Results, para. 4). The mirror was a concave gold-surfaced copper mirror having a 2-m radius of curvature. The output coupler was a 95% reflective germanium flat that was antireflection coated on one surface.

The multiline laser beam consisted of up to six lines of the HF vibrational-rotational spectrum. The beam is shown analyzed in Fig. 1 by the rotating-grating spectrometer that scanned the dispersed lines serially, once per second, across an InAs room-temperature detector D5. All detectors had amplifiers with resultant frequency response of > 30 kHz. The spectrum was displayed on scope 3. Detector D4 was used to monitor fluctuations in total power (see Results, para. 4). Sanded salt windows S3 and S4 were used to diffuse the beam to keep detectors and amplifiers within their linear regime of sensitivity. Beam power at the laser was 3 W with a diameter of 2 mm and a divergence of 2 mrad.

Half of the power was diverted by beam splitter B5 for analysis. The other half entered the MZ through beam splitter B1. This and B2 were 3-in. diameter zinc selenide flats that were antireflection coated on one side and dielectrically coated on the other side for 50% reflectivity at  $\lambda = 2.7 \mu\text{m}$  and 30 degrees angle of incidence. Hence the incident beam was split into two identical beams at the front surface of B1. The two beams were then reflected by gold-surfaced mirrors M1 and M2. Mirror M2 was scannable over several centimeters<sup>1</sup> by a translation mount fitted with a micrometer screw drive that could be turned uniformly by a 480-rpm synchronous motor. This mirror was also scannable electronically about 8  $\mu\text{m}$  in response to 0-1000-V dc input to its PZT mirror mount. Each beam was again split in two at the reflective sur-

face of B2. To align the MZ, its optical elements were adjusted while diffuse light from an extended-source sodium arc lamp was viewed through the MZ. Infinite fringes of uniform intensity observed at the exit aperture, and at a distance of 2 m from it, ensured superposition of the outgoing beams in both MZ exits.

The intensities  $I^+$  and  $I^-$  of the two beams were measured by detectors D1 and D2 and displayed on oscilloscopes 1 (upper trace on scope 1, Fig. 1) and 2 (lower trace on scope 2, Fig. 1). OPD was varied uniformly at 7 mm/s (4 mm/s mirror movement) and a scan of the multiline interference fringes through zero OPD was produced and recorded on scope 1. From this record (see Results, paras. 6 and 7), fringe intensities could be measured and visibilities calculated. Adjustment of the MZ to zero OPD was checked by producing white light fringes using collimated light from a zirconium arc source. The white-light fringes were visible to the eye and were detected by a 1P28 photomultiplier to produce a fringe record. White-light zero OPD was about 13 IR fringes, or about 35  $\mu\text{m}$  OPD, from the IR zero-OPD position; this results because beam splitters B1 and B2 differ slightly in thickness, which creates an effective dispersion mismatch between the white light and the IR beams. To set the MZ to zero OPD, the mirror was moved from the white-light zero-OPD thirteen IR fringes to the IR zero-OPD position. Infrared fringe intensities were monitored on the scope. This process caused the beams to be shifted laterally about 20  $\mu\text{m}$  from their established collinearity. Single-line fringe scans show that this did not decrease fringe visibility. The beam width was about 5 mm in diameter (FWHM) at the MZ exit.

The array spectrometer was an Optical Engineering, Inc. model 16-8 laser spectrum analyzer with a specially made array of InAs detectors and amplifiers fixed to its output. The beam was focused by a 22-cm radius-of-curvature aluminum-surfaced mirror through the entrance slit of the spectrometer to a grating that dispersed the various lines, each to its own detector. This gave a continuous reading of the direct-exit intensity  $I_1^+$  on each line. These intensities were still subject to MZ OPD and produced single-line fringe-intensity scans when OPD was scanned (see Results, paras. 6 and 7). Hence the

single-line and multiline fringe scans were produced simultaneously. Each array detector had its own amplifier that required calibration. Calibration was done by means of a continuous spectrum that was recorded from the array simultaneously with a single-sweep spectrum from the rotating-grating spectrometer.

The MZ was constructed with a laser amplifier in one leg. This was the gain region of the Aerospace supersonic-diffusion HF laser fitted with a 36-slit nozzle of gain length  $L = 17$  cm. The beam was centered at  $X_c = 1.0$  cm downstream from the nozzle exit, which gave a gain of about 12% per cm on some lines.<sup>8</sup> The beam diameter was about 4 mm at the nozzle, which gave an average input intensity of about  $5 \text{ W/cm}^2$ . Compensation for the amplifier windows was provided by two  $\text{CaF}_2$  windows in the other leg of the MZ. This made it possible to use white-light fringes for alignment. All four windows were approximately perpendicular to the optical axes.

The phase-lock system consisted of an Infrasil-plate beam splitter B4, an InAs detector D3, a lock-in amplifier (PAR model 128A), a sine-wave generator, a zero-gain operational-amplifier mixer (Tektronix type-O plug-in unit), a high-voltage operational amplifier (Burleigh PZ-70), a PZT mirror driver (Burleigh PZ-80), and the MZ itself, the output intensities of which were functions of OPD and, therefore, of the position of the MZ PZT-driven mirror. The object of the control loop was to minimize continuously the indirect output intensity  $I^-$  from the MZ. A sample of  $I^-$  was taken by B4 and monitored by D3. Infinite fringes of zero intensity in the indirect exit implied phase matching in the direct exit of the MZ.

The sine-wave signal of 0.3-V-peak-to-peak amplitude and frequency  $f = 500$  Hz was amplified to 60 V by the PZ-70. This gave the PZT-driven MZ mirror an axial oscillation of about  $0.3 \mu\text{m}$  peak to peak and varied OPD in the MZ by about  $0.5 \mu\text{m}$  peak to peak, or about  $\frac{\lambda}{5}$ , at frequency  $f$ . Ideally zero OPD would be traversed at frequency  $2f$ , and a near-zero intensity  $I^-$  would be modulated at frequency  $2f$ ; the signal produced by D3 would not be amplified by the PAR referenced to the sine wave of frequency  $f = 500$  Hz. However, when OPD in the MZ changed because of optical system variations, the modulation of

$I^-$  would increase in the 500-Hz component. The phase of the modulation relative to the reference sine wave gave an algebraic sign to the OPD change. This component of the signal from D3 was amplified by the PAR, mixed with the dither sine wave, and impressed on the PZT mirror driver to correct the OPD change. This hill-climbing action continuously minimized  $I^-$  as long as the OPD change was not too sudden and not more than about 5  $\mu\text{m}$ , or half the maximum translation capability of the PZ-80.

Thus the MZ was locked to a fringe. Locking to the central multiline fringe held the MZ at zero OPD. Adjustment of the MZ to the central fringe was tested by varying the spectral content of the probe-laser beam and observing a quiescent control signal taken from the PZ-70 low-voltage output (HV + 100).

To test locking response, the control loop was alternately opened and closed by chopping the beam to D3 at 28 cps.

#### IV. RESULTS

The results of locking the MZ to the central fringe are shown without gain ( $g = 0$ ) in Fig. 2a. Note the  $2f$  modulation of  $I^-(0)$ .

Locking with gain  $g$  is shown in Fig. 2b. Average gain  $g = 0.06/\text{cm}$  can be calculated from Eq. (9), assuming single-line radiation, since  $I^+(0)_{\text{max}} = I^+(0) = I$  from Fig. 2a. Gain increased  $I^-$  only slightly, in accordance with Eq. (16).

The response of the locking system to chopping the control loop is shown in Fig. 3. Figure 3a shows a good  $2f$  modulation of  $I^-$  when the loop is closed. Figure 3b shows frequency- $f$  modulation of  $I^-$  and therefore poor locking. It also shows jumping between fringes. This gives a calibration of the fringe spacing of  $320 \text{ V}$  applied to the PZT mirror driver. Locking was attained in about  $5 \text{ ms}$  for a small OPD correction of about  $\frac{\lambda}{6}$  in Fig. 3a.

Figure 4a shows line-switching induced by a ramp voltage impressed on the PZT of the probe laser cavity. Figure 4b shows the effect of this two-line input on the locking system with the MZ adjusted to zero OPD. Figure 4c shows the effect of this input on locking with the MZ adjusted off zero OPD. Note the erratic response of the control signal and  $I^-$ . This erratic response to induced changes in the spectral output of the probe laser was used to determine when OPD was not zero. Jumping fringes to find a quiescent signal was a means of locating zero OPD to within  $\pm 2$  fringes, without recourse to visible fringes.

Figure 5 shows, in the top six traces, the individual spectral-line intensities as monitored continuously by the array spectrometer. Voltage on each trace is measured downward from the baseline for that trace. Note the oscilloscope-channel sensitivities listed at left. The bottom trace shows a simultaneous spectrum recorded from the rotating grating. This and similar photos were used to calibrate the array spectrometer. The calibration coefficients  $C_1$  are given in Table 1.

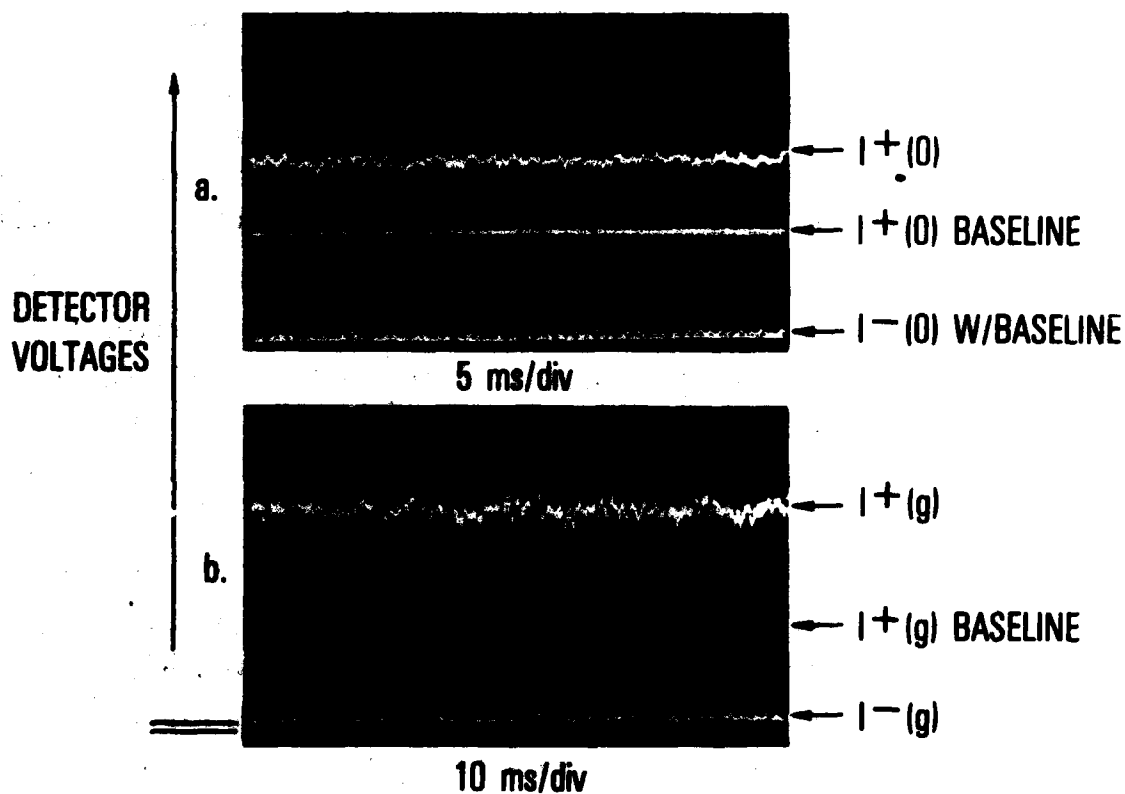


Fig. 2. (a) Multiline Fringe Intensities  $I^+(g = 0)$  and  $I^-(g = 0)$  Locking without Gain. Relative intensity is measured upward from baselines ( $I = 0$ ). (b) Multiline Fringe Intensities  $I^+(g)$  and  $I^-(g)$  Locking with Gain (amplifier on). Baselines are the same as in (a), above.

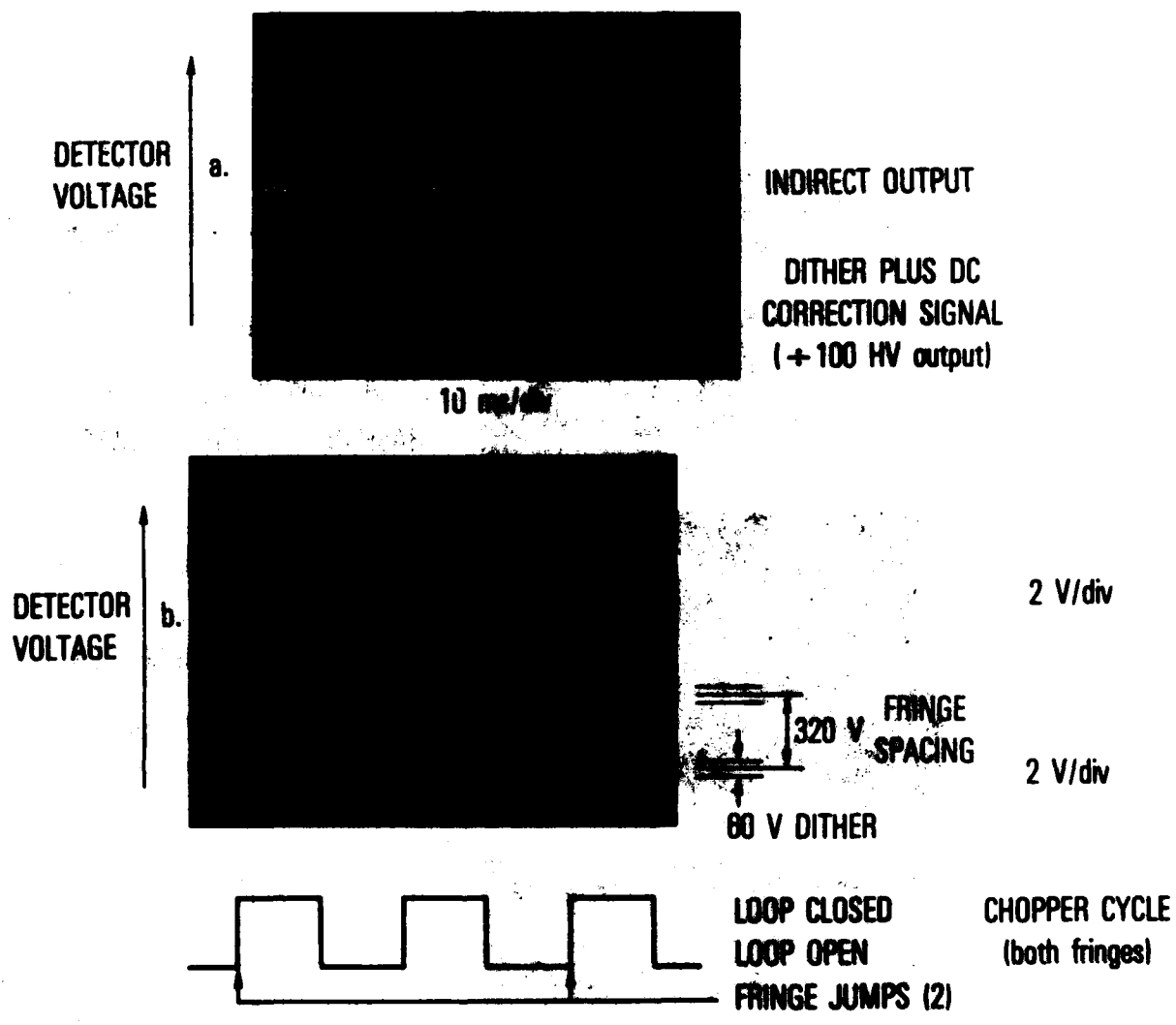


Fig. 3. (a) Chopping of Control Loop and Attainment of Locking;  
 (b) Locking on Two Different Fringes



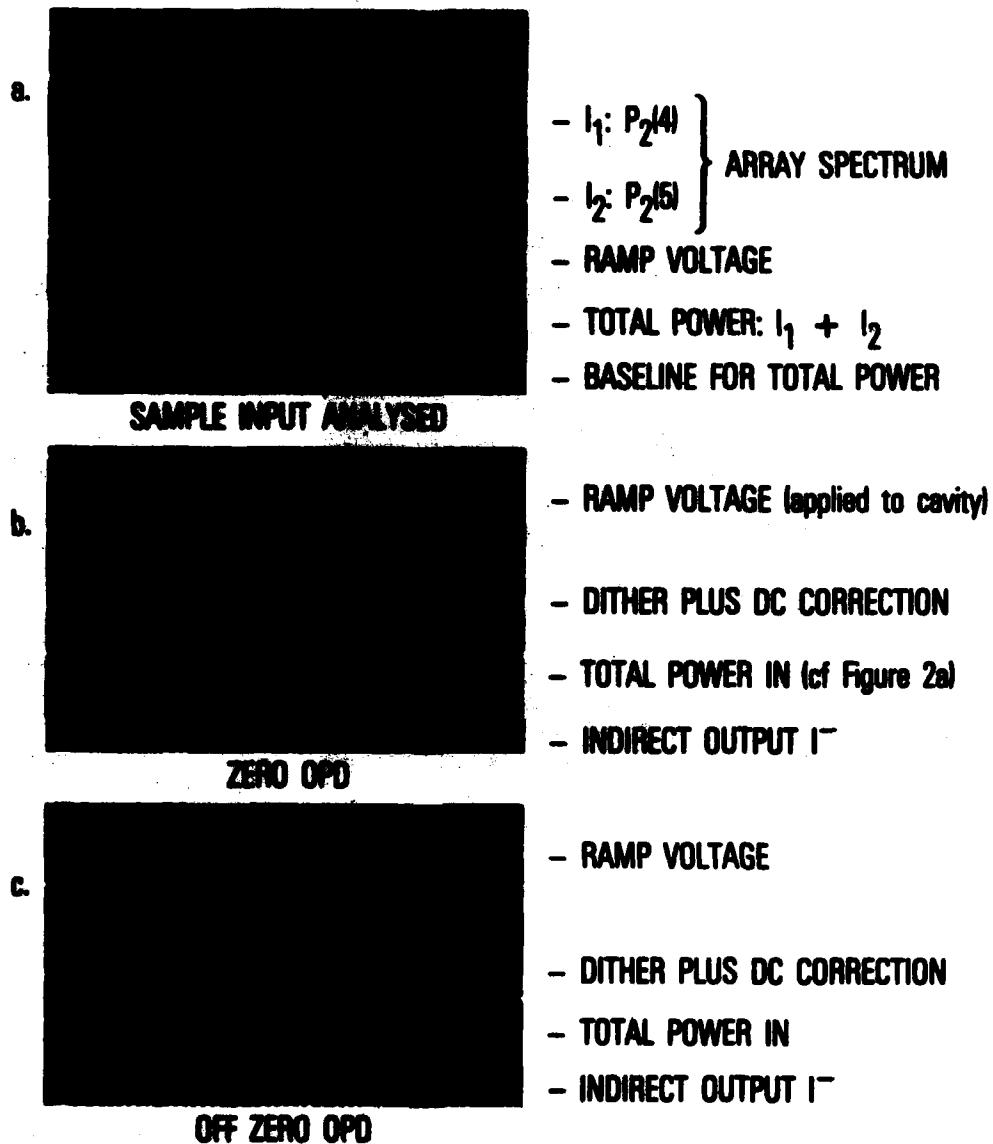


Fig. 4. (a) Induced Line Switching (ILS) Analyzed; (b) Effect of ILS at Zero OPD; (c) Effect of ILS off Zero OPD

1.00 V/div P<sub>1</sub>(4) -  
0.05 V/div P<sub>1</sub>(5) -  
0.20 V/div P<sub>1</sub>(6) -  
0.05 V/div P<sub>2</sub>(4) -  
0.50 V/div P<sub>2</sub>(5) -  
0.50 V/div P<sub>2</sub>(6) -



P<sub>2</sub>(6) P<sub>2</sub>(5) P<sub>2</sub>(4) P<sub>1</sub>(6) P<sub>1</sub>(5) P<sub>1</sub>(4)

Fig. 5. Comparison of Rotating Grating with Array Spectrometer

Table 1. Calibration Coefficients  $C_i$

i	1		2		3		$C_i$ (avg) Norm
	$I_i$ (rel) RG (V)	$I_i$ (rel) Array (V)	$I_i$ (rel) RG	$I_i$ (rel) Array	$I_i$ (rel) RG	$I_i$ (rel) Array	
1	1.0	0.25	1.5	0.25	0.9	0.20	1.0
2	0.06	0.005	0	0	0.12	0.012	2.3
3	1.60	0.07	0.75	0.03	0.70	0.03	4.7
4	0	0	0	0	0	0	---
5	0.30	0.08	0.60	0.13	0.60	0.13	0.9
6	1.30	0.23	0.75	0.11	0.55	0.10	1.2

Figure 6 shows the single-line fringe scans without gain as recorded by the array spectrometer. Note the visibility  $V = 1.0$  for all scans. A simultaneously recorded multiline fringe scan is also shown. In the multiline scan (upper photo), fringe intensity is measured upward from the baseline. The upper trace shows a blip of white-light fringes. The intensity of the single-line fringes is measured downward from the baseline for each scan.

Figures 7 and 8 show single-line and multiline fringe scans with gain (arc laser amplifier on). Baselines for the multiline fringe scans are indicated and are the same as for Fig. 6. Visibilities of the central fringes were calculated and compared as follows:

Multiline	Single-line
Figure 7: $V = 0.81 \pm 0.02$	$\frac{\Sigma I_{\max} - \Sigma I_{\min}}{\Sigma I_{\max} + \Sigma I_{\min}} = 0.80 \pm 0.13$
Figure 8: $V = 0.83 \pm 0.02$	$\frac{\Sigma I_{\max} - \Sigma I_{\min}}{\Sigma I_{\max} + \Sigma I_{\min}} = 0.82 \pm 0.08$

From this result it was concluded that dispersion in our amplifier was negligible for the probe-laser input used.

The effect of gain on phase-locking was not tested beyond observing that locking continued when the amplifier was on.

ARC OFF

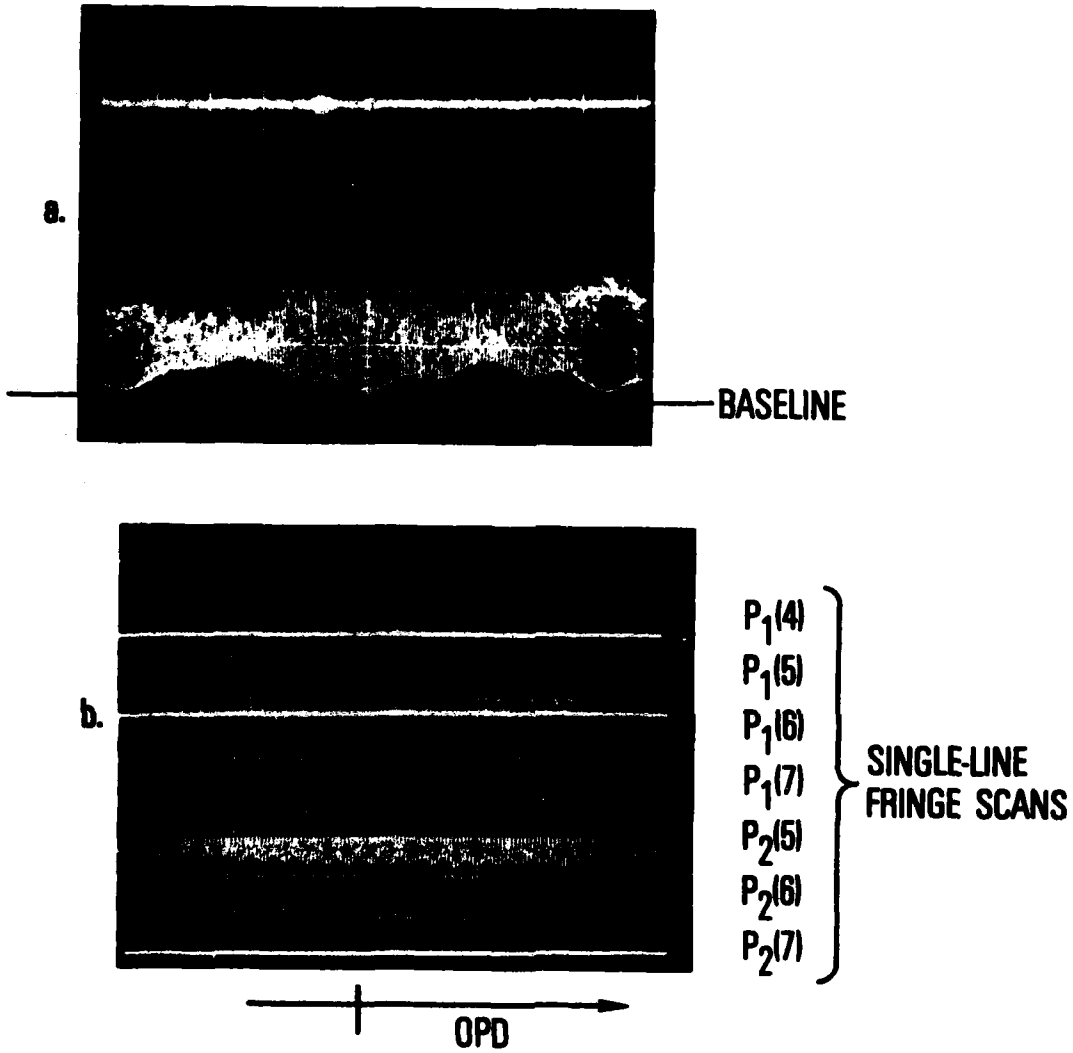
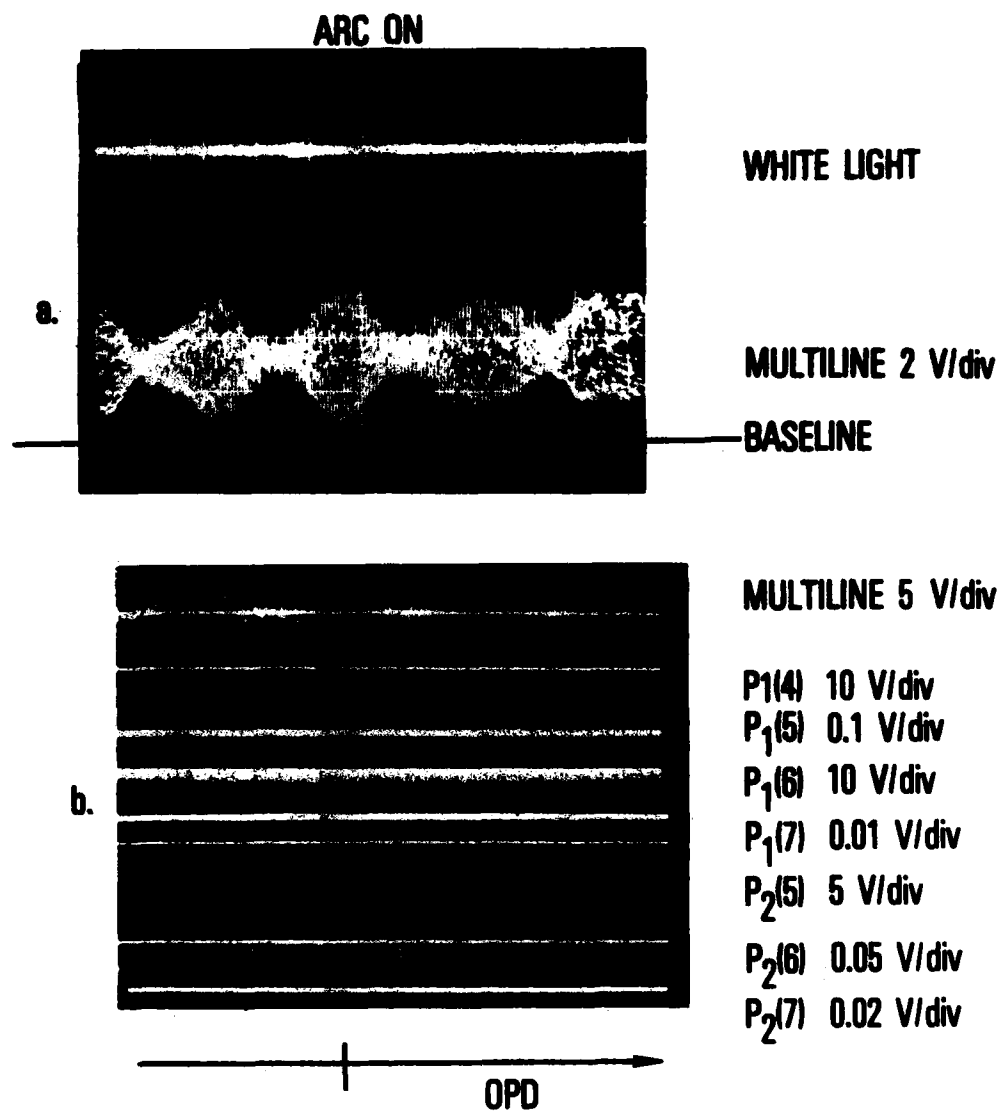
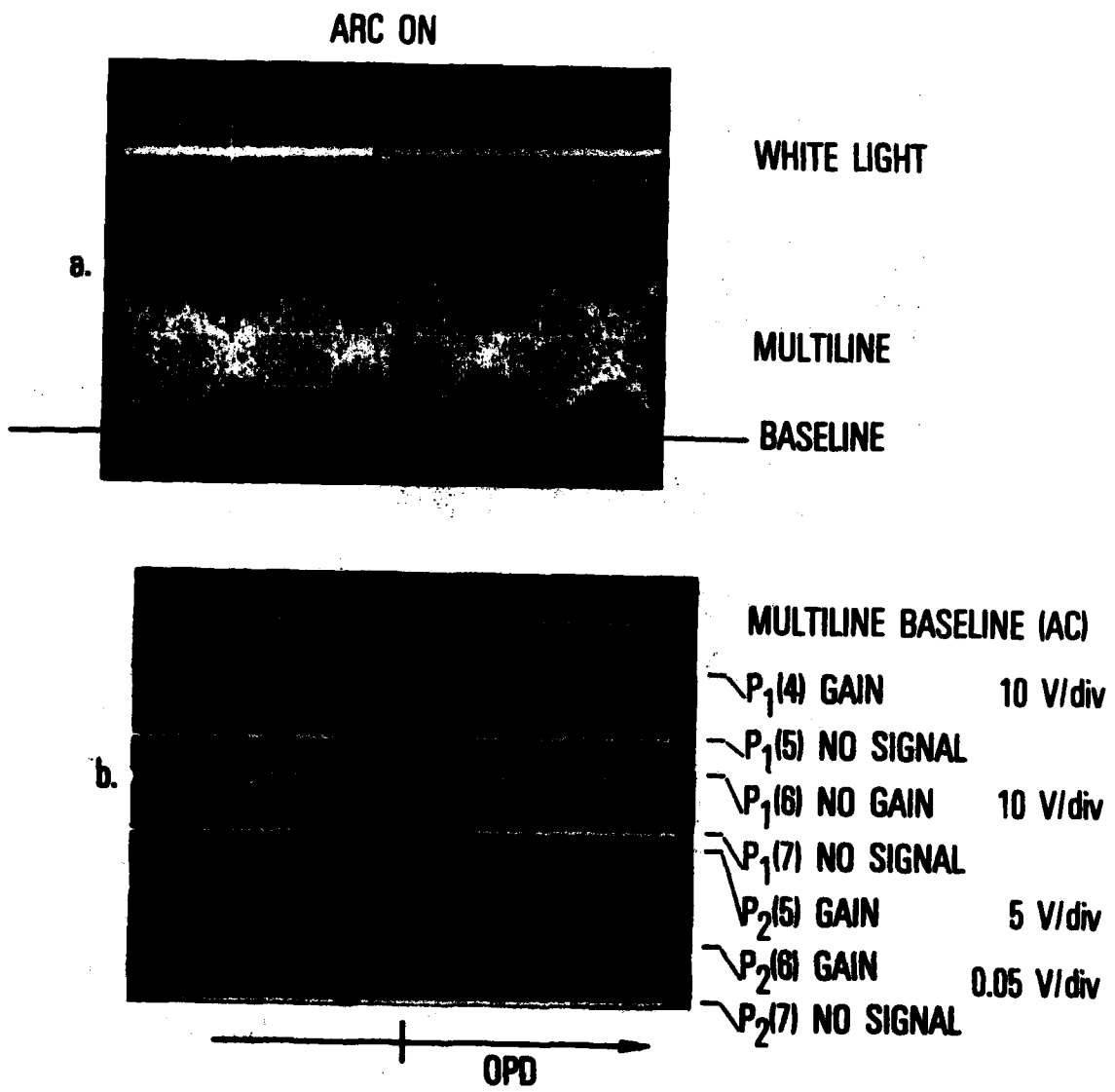


Fig. 6. Scan of Multiline Interference Fringes through Zero OPD, Laser Amplifier Power Off



**Fig. 7. Scan of Multilane Interference Fringes through Zero OPD, Laser Amplifier Power On**



**Fig. 8. Scan of Multiline Interference Fringes through Zero OPD, Laser Amplifier Power On**

## V. CONCLUSIONS

Continuous phase matching of multiline HF-laser beams split off from one parent beam was demonstrated in principle by means of a phase-locked, Mach-Zehnder interferometer. Two collinear beams in the direct exit of the MZ were continuously phase-matched when the intensity out of the indirect exit was held to a minimum by a mirror-dither, hill-climbing servo system operating at a dither frequency of 500 Hz. This held OPD in the MZ to  $\pm \frac{\lambda}{10}$  about zero OPD. For a given spectral input, the interferometer could be locked to any value of OPD where there was an interference-intensity minimum in the indirect exit. Varying the spectral input when locking off zero OPD produced erratic locking. At zero OPD, variations in spectral input had no effect on locking. This effect was used to check that the interferometer was locked to the central fringe. The response of the system to opening the feedback control loop was tested. When the loop was reclosed, locking was recovered in less than 5 ms for a drift of  $\frac{\lambda}{6}$  OPD. Amplification of one beam within the MZ was found to have little effect on locking, even though central-fringe visibility was decreased.

An array spectrometer was used to monitor single-line interference intensities in the direct exit while scanning OPD. This was done to measure typical laser spectral content and amplifier gain on each line. Equations were developed to measure the gain from single-line fringe visibility.

Resonant dispersion in the amplifier was found to have no observable effect in this system. This was demonstrated by comparing the visibility of the multiline central fringe with the intensities of the additive component single-line central fringes. Here measurements were made on the assumption that the central fringe was the middle of the central lobe of fringes. This assumption is not entirely justified since resonant dispersion could possibly induce an OPD shift in the central lobe without decreasing visibility at the center of the lobe. Our fringe records were not accurate enough to show the absence or presence of such an OPD shift.



It is our contention that, with more accuracy and better coincidence of recording of the single-line fringes, any significant shift of the central lobe caused by dispersion could be observed. This technique may thus be applicable to testing the degree to which two larger amplifiers are matched in their dispersion and act as compensators for each other. It can be used in the absence of any system for actively controlling phase.

A final system for phase matching of parallel amplified multiline laser beams would require specifications of frequency response, which may require a higher dither frequency and larger path length correction capability to respond to high-frequency large-amplitude system vibrations. Rapid fluctuations in gain that are uncorrelated with input-beam spectral content would have to be addressed in amplifier design. Our measurements of gain were done at a rate of about 300 Hz and showed gain to vary slowly, which implies that dispersion also varies slowly. Fluctuations in gain and dispersion that are correlated with input-beam spectral content should produce compensatory phase shifts in identical amplifiers driven by identical inputs and should result in a visibility of unity for the central multiline fringe.

Gain-measurement frequency can be increased by increasing mirror-scan speed.

The accuracy of comparison of multiline and single-line visibilities is limited by the physical dimensions of the recorded traces and can be vastly improved.

Phase-lock circuitry can be tuned to give greater response by employing a higher dither frequency. This is limited by PZT resonances that are higher than 2000 Hz in some systems.<sup>9</sup> Adjusting mixer gains from zero would also improve locking response.<sup>9</sup>

Two amplifiers like the one employed in these experiments might exhibit dispersion mismatch that would observably affect the visibility of the central fringe, and thereby the ability of a more sensitive phase-lock system to continuously match the phases of the multiline output. It seems likely that two larger amplifiers can be made to match as well as our gain leg matched our zero-gain leg.

## REFERENCES

1. R. W. F. Gross, J. G. Coffey, R. A. Chodzko, and E. B. Turner, "Interference Patterns Produced by a Mach-Zehnder Interferometer and a Multiline HF Laser," TR-0080(5764-2), The Aerospace Corporation, El Segundo, Calif. 90245.
2. W. R. Warren, "The Parallel Internal-Master-Oscillator Power Amplifier for Phase Matching the Output Beams of Multiline Lasers," TR-0078(9990)-6, The Aerospace Corporation, El Segundo, Calif. 90245.
3. A. A. Michelson, Light Waves and Their Uses, The University of Chicago Press, Chicago, 1907.
4. T. R. O'Meara, "The Multidither Principle in Adaptive Optics," J. Opt. Soc. Am. 67, No. 3 (306-307), March 1977.
5. M. Born and E. Wolf, Principles of Optics, 5th Edition, Pergamon Press, Oxford, 1975.
6. R. W. F. Gross, R. Chodzko, E. B. Turner, and J. G. Coffey, "Measurements of the Anomalous Dispersion of HF in Absorption," TR-0079(4764)-2, The Aerospace Corporation, El Segundo, Calif. 90245.
7. D. J. Spencer, J. A. Beggs, and H. Mirels, "Small-Scale HF(DF) Chemical Laser," J. Appl. Phys. 48, 1206 (1977).
8. R. A. Chodzko, D. J. Spencer, H. Mirels, S. B. Mason, and D. H. Ross, "Zero-Power-Gain Measurements in CW HF(DF) Laser by Means of Fast-Scan Technique," IEEE J. Quant. Elec., Vol. QE-12, No. 11, November 1976.
9. R. L. Varwig and C. P. Wang, private communication.

## LABORATORY OPERATIONS

The Laboratory Operations of The Aerospace Corporation is conducting experimental and theoretical investigations necessary for the evaluation and application of scientific advances to new military space systems. Versatility and flexibility have been developed to a high degree by the laboratory personnel in dealing with the many problems encountered in the nation's rapidly developing space systems. Expertise in the latest scientific developments is vital to the accomplishment of tasks related to these problems. The laboratories that contribute to this research are:

Aerophysics Laboratory: Launch vehicle and reentry aerodynamics and heat transfer, propulsion chemistry and fluid mechanics, structural mechanics, flight dynamics; high-temperature thermomechanics, gas kinetics and radiation; research in environmental chemistry and contamination; cw and pulsed chemical laser development including chemical kinetics, spectroscopy, optical resonators and beam pointing, atmospheric propagation, laser effects and countermeasures.

Chemistry and Physics Laboratory: Atmospheric chemical reactions, atmospheric optics, light scattering, state-specific chemical reactions and radiation transport in rocket plumes, applied laser spectroscopy, laser chemistry, battery electrochemistry, space vacuum and radiation effects on materials, lubrication and surface phenomena, thermionic emission, photosensitive materials and detectors, atomic frequency standards, and bioenvironmental research and monitoring.

Electronics Research Laboratory: Microelectronics, GaAs low-noise and power devices, semiconductor lasers, electromagnetic and optical propagation phenomena, quantum electronics, laser communications, lidar, and electro-optics; communication sciences, applied electronics, semiconductor crystal and device physics, radiometric imaging; millimeter-wave and microwave technology.

Information Sciences Research Office: Program verification, program translation, performance-sensitive system design, distributed architectures for spaceborne computers, fault-tolerant computer systems, artificial intelligence, and microelectronics applications.

Materials Sciences Laboratory: Development of new materials: metal matrix composites, polymers, and new forms of carbon; component failure analysis and reliability; fracture mechanics and stress corrosion; evaluation of materials in space environment; materials performance in space transportation systems; analysis of systems vulnerability and survivability in enemy-induced environments.

Space Sciences Laboratory: Atmospheric and ionospheric physics, radiation from the atmosphere, density and composition of the upper atmosphere, aurorae and airglow; magnetospheric physics, cosmic rays, generation and propagation of plasma waves in the magnetosphere; solar physics, infrared astronomy; the effects of nuclear explosions, magnetic storms, and solar activity on the earth's atmosphere, ionosphere, and magnetosphere; the effects of optical, electromagnetic, and particulate radiations in space on space systems.

**END**

**FILMED**

**1-84**

**DTIC**